Effects of Surface Chemistry on Aromatic Compound Adsorption from Dilute Aqueous Solutions by Activated Carbon

F. Haghseresht,[†] S. Nouri,[‡] J. J. Finnerty,[†] and G. Q. Lu*[,†]

The Nanomaterials Centre and Department of Chemical Engineering, University of Queensland, Brisbane, QLD 4072, Australia, and Chemistry Department, Urumieh University, Urumieh, Iran

Received: January 15, 2002; In Final Form: July 26, 2002

Adsorption of one nondissociating and four dissociating aromatic compounds onto three untreated activated carbons from dilute aqueous solutions were investigated. All adsorption experiments were preformed in pH-controlled solutions. The experimental isotherms were analyzed using the homogeneous Langmuir model. The surface chemical properties of the activated carbons were characterized using a combination of water adsorption, X-ray photoemission spectroscopy, and mass titration. These data give rise to a new insight into the adsorption mechanism of aromatic solutes, in their molecular and ionic forms, onto untreated activated carbons. It was found that, for the hydrophilic activated carbons, the dominant adsorption forces were observed to be dipolar interactions when the solutes were in their molecular form whereas dispersive forces, such as $\pi-\pi$ interactions, were most likely dominant in the case of the basic hydrophobic carbons. However, when the solutes were in their ionic form adsorption occurs in all cases through dispersive forces.

1. Introduction

Due to their widespread use as ingredients and solvents in various manufacturing industries, aromatic compounds are common water contaminants. Most of these compounds are recognized toxic carcinogens. With increasing environmental awareness, the regulations on the acceptable levels of these compounds have become more stringent. This has led to a growing interest in removing these compounds from water. Aeration, biological degradation, and adsorption are well-known among the various methods that are available for the removal of aromatic compounds. Of these methods, adsorption is still the preferred method as it can be used for the removal of a variety of organic compounds.[1,2]

In liquid-phase adsorption, it has been established that the adsorption capacity of an activated carbon depends on a number of factors: first, the physical nature of the adsorbent-pore structure, ash content, and functional groups;[3−7] second, the nature of the adsorbate, its pK_a, functional groups present, polarity, molecular weight, and size;[8−15] finally, the solution conditions such as pH, ionic strength, and the adsorbate concentration.[16,17] Despite extensive studies reported in the literature on the factors influencing the adsorption process, the mechanism of the adsorption is still not well understood and subject to much debate.

The literature shows several theories attempting to explain the adsorption mechanism. One of the theories suggested that aromatic compounds are adsorbed through sorbate−sorbent $\pi-\pi$ interactions. This model, initially suggested by Coughlin and Ezra[8] and supported by recent researchers,[18] is based on the traditional understanding of $\pi-\pi$ interactions as proposed in classical organic chemistry literature.[19] The facedown orientation for $\pi-\pi$ interactions is derived from the adsorption of aromatic and aliphatic compounds onto a mercury surface reported in the 1960s by Barradas and co-workers.[20] This theory predicted that any modification that leads to depletion of the surface density of the π electrons, such as oxidation or nitriding, caused a decrease in the solute uptake. Conversely, modifications involving the removal of the surface electron withdrawing atoms, such as oxygen, cause an increase in the solute uptake. Another theory reported by Mattson et al.[10] suggested that adsorption occurs through the formation of an electron donor−acceptor complex between the aromatic compounds and the carbonyl groups present on activated carbon. However, this type of interaction has been reported to be insignificant by authors such as Franz et al.[15]

Although it is accepted that the nature of the solute affects the adsorption process, the effects of other possible sorbate−sorbent interactions, such as dipolar interactions have not been considered in the literature. In this work, the adsorption isotherms of five aromatic compounds on three untreated commercial carbons are investigated systematically. All isotherms were obtained in pH-controlled solutions. The experimental isotherms are fitted to the homogeneous Langmuir model. The physical and chemical properties of the activated carbon are characterized using gas and vapor adsorption, mass titration, and XPS data. Characteristic parameters of the pore structure and the surface chemistry of the activated carbons and selected chemical properties of the solutes are presented. These properties together are used to propose a new insight into the adsorption mechanism of the molecular and ionic forms of aromatic solutes onto activated carbons.

2. Analysis of the Adsorption Data

2.1. Characterization from N_2 and CO_2 Data. The nitrogen adsorption data were used to determine the BET surface areas (S_{BET}), the total pore volumes (V_{tot}) and the micropore volumes (V_{mic}) of the activated carbons. The BET surface area was obtained by applying the BET equation to the adsorption data in the P/P_0 range 0.01−0.1, V_{tot} was obtained from the adsorption at $P/P_0 = 0.96$, and the micropore volume, V_{mic}, was

* Corresponding author:. Fax: +61 7 33654199. E-mail: m.lu@uq.edu.au.
[†] University of Queensland.
[‡] Urumieh University.

10.1021/jp025522a CCC: $22.00
Published on Web 10/01/2002

obtained using the t-plot method.[21] The ultramicropores volumes (V_{ulmic}) of the carbons were obtained by applying the Dubinin−Radushkevich equation (DR) to CO_2 adsorption isotherms obtained at 273 K.[22,23]

2.2. Toluene and Water Adsorption. Toluene pore volumes of the activated carbons were determined by using the monolayer adsorption capacity of the activated carbons for toluene and using 0.866 g cm^{-3} [24] as the toluene density.

The water adsorption data were analyzed by fitting the water adsorption isotherms to eq 1, the DS-2 equation.[25]

$$c(Q_0 - q)(1 - kq) = q/(P/P_0) \tag{1}$$

where q is the measured adsorption amount per gram of the carbon, P/P_0 is the relative pressure, c is the kinetic parameter, k is the constant involved in decreasing active site concentration, and Q_0 is the concentration of the primary sites.

2.3. Adsorption of the Aromatic Compounds from Aqueous Solutions. The monolayer adsorption capacities of the carbons were determined using the homogeneous binary Langmuir equation (eq 2a).

$$\frac{C_{eq}}{q} = \frac{(1+\alpha)}{(K_m + K_i\alpha)Q_{max}} + \frac{1}{Q_{max}}C_{eq} \tag{2a}$$

where

$$\alpha = \frac{C_i}{C_m} \quad \text{and} \quad pH - pK_a = \log(\alpha) \tag{2b}$$

$$K_l = \frac{K_m + K_i\alpha}{1+\alpha} \tag{2c}$$

$C_{m,i}$ are the concentrations of the molecular and ionic species, respectively, C_{eq} is total concentration of the ionic and molecular species at equilibrium, q is the adsorbed amount in millimoles per gram of the carbon, Q_{max} is the monolayer capacity of the carbon, K_l is the lumped equilibrium constant of the molecular and ionic species, and $K_{m,i}$ is the equilibrium constant of the molecular and ionic species, respectively.

In an adsorption system where the molecular species are dominant, eq 2a would simplify to the single solute Langmuir equation. The plot of C_{eq}/q versus C_{eq} would then lead to the determination of the monolayer adsorption capacity, Q_{max}, and the molecular affinity coefficient, K_m, from the slope and the intercept, respectively. However, when adsorption is carried out in solution pH where both the molecular and ionic species are present, the fitted equilibrium constant K_l would be a lumped parameter containing K_m, K_i, and α. A similar approach was also employed by Getzen and Ward.[26] Furthermore, eq 2c can be rewritten in its linear form (eq 2d), which shows the relationship between the lumped affinity coefficient and those of the molecular and ionic species.

$$K_l + K_l\alpha = K_m + K_i\alpha \tag{2d}$$

2.4. Test of Correlation for the Effects of the Solute Properties. To test the significance of observed relationships, the correlation coefficient (r)[27] of selected important properties of the solutes, such as their pK_a and dipole moments, and the calculated adsorption parameters are calculated. Using the *t*-test, the minimum value of r, which shows a significant linear relationship between two given sets of data for $n = 5$ (the number of data points) and in limited cases for $n = 4$ are determined at 0.05 significance. Utilizing the corresponding critical t values for a given n (3.18 and 4.3, respectively[27]) the minimum r values for $n = 4$ and 5 are determined to be 0.902 and 0.771, respectively.

3. Experimental Section

3.1. Materials. The activated carbons used in this study were BDH, F100, and SEI, supplied by Merck, Calgon Corp. and a local supplier, respectively. Of these carbons, BDH is coconut shell-based and the other two are coal-based carbons. The chemicals were benzoic acid (BA), *p*-nitrophenol (PNP), *p*-cresol (PC), and nitrobenzene (NB) supplied from Merck. The purity of all chemicals was either the synthesis or analytical grade.

3.2. Gas Adsorption. Nitrogen adsorption/desorption experiments were carried out manometrically at 77 K using an Autosorb (Quantachrome Corp.). Carbon dioxide adsorption experiments were also carried out manometrically, at 273 K, using NOVA 1200 (Quantachrome Corp.). All samples were degassed overnight at 200 °C, prior to the adsorption experiments.

3.3. Vapor Adsorption. Toluene and water adsorption experiments were carried out gravimetrically using an in-house adsorption apparatus equipped with quartz springs, a MKS transducer, measuring absolute pressure with the precision of ±1 mTorr, and a temperature controlled oven, capable of heating to 200 °C. Prior to the adsorption experiments, all samples were degassed overnight at 150 °C. A lower degassing temperature was used than that of the gas adsorption experiments. This was for maintaining the integrity of the surface oxides, as these functional groups affect the observed water adsorption behavior significantly. In these experiments, the samples were subjected to a step change in the sorbate pressure from the initial zero to its saturation pressure.

3.4. XPS Characterization. XPS measurements were conducted with a PHI-Model 560 ESCA system (Perkin Elmer) that employed a model 25-270 AR cylindrical mirror analyzer. All spectra were acquired at a basic pressure of 2×10^{-7} Torr with Mg Kα excitation and 400 W. Survey (wide) scans were recorded with pass energy of 100 eV and multiplex (narrow) scans, over selected elemental regions, at 50 eV pass energy. Because of sample charging, binding energies were referenced to carbon (1s) at 285 eV.[28] Elemental concentrations were calculated after correction of the peak areas for atomic sensitivity factors.[29]

3.5. Determination of Point of Zero Charge (pH_{PZC}). The pH_{PZC} of the carbon was determined as suggested by Noh et al.[30] This was done by placing various amounts of the carbon in a 10 mL solution of 0.1 M NaCl (prepared in preboiled water to eliminate CO_2). The bottles were sealed to eliminate any contact with air. They were then placed in a thermostat shaker overnight. The equilibrium pH values of the mixtures were then measured. The limiting pH was taken as the pH_{PZC}.

3.6. Equilibrium Studies. The adsorption experiments were carried out by placing 45 mg of the activated carbon into 50 mL of the solution containing different concentrations of the adsorbates. Solution pH conditions were adjusted using dilute NaOH or HCl. All solutions were then left in Thermostat shaking bath for 4 days at 301 K to reach equilibrium. After reaching equilibrium conditions, the residue concentrations of the solutes were then measured spectrophotometrically, using JASCO-V550 spectrophotometer.

4. Results and Discussion

4.1. Characterization of the Activated Carbons. *4.1.1. Pore Structures of the Activated Carbons.* Nitrogen adsorption/desorption isotherms, together with the adsorption isotherms of

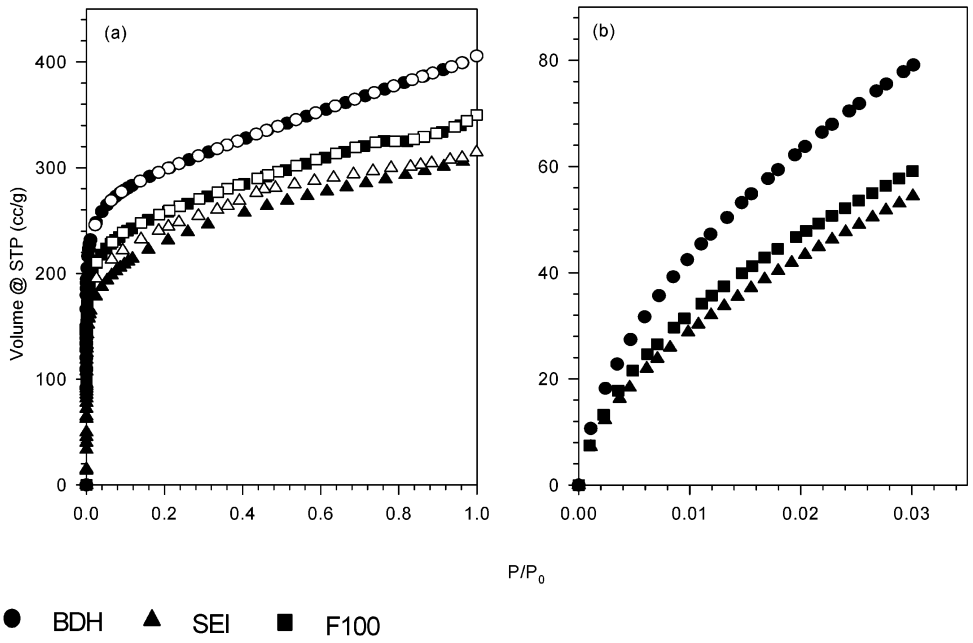

Figure 1. (a) N_2 Adsorption/desorption and (b) CO_2 adsorption isotherms of BDH, SEI and F100. Empty symbols represent the desorption branch.

TABLE 1: Pore Structure Properties of the Activated Carbons Determined by Using N_2, CO_2, and Toluene Adsorption Data

solute	S_{BET} ‘($m^2\ g^{-1}$)	V_{tot} ($cm^3\ g^{-1}$)	V_{mic} ($cm^3\ g^{-1}$)	V_{ulmic} ($cm^3\ g^{-1}$)	V_{tol} ($cm^3\ g^{-1}$)
BDH	1118	0.618	0.416	0.282	0.28
F100	957	0.526	0.381	0.207	0.27
SEI	827	0.474	0.344	0.197	0. 30

CO_2 of all three carbons are shown in Figure 1a,b, respectively. The N_2 adsorption data are used to determine standard pore structure characteristics of the carbons, such as their BET surface area (S_{BET}) and total pore volume (V_{tot}). In addition, the CO_2 adsorption data are used to gain insights into the structure of finer microspores (ultramicropores, V_{ulmic}), supplementing the N_2 adsorption data.

As illustrated in Figure 1a, the N_2 adsorption isotherms of all activated carbons show a rapid rise in adsorption in low relative pressure followed by a plateau, characteristic of type I isotherms.[31] This figure also shows that adsorption/desorption isotherms of SEI exhibit a small hysteresis persisting to low pressures. The presence of hysteresis is an indication of the presence of mesoporosity, and its persistence to low pressures indicates a small degree of pore constriction.[21]

Using the N_2 and CO_2 adsorption data, the S_{BET}, V_{tot}, and V_{ulmic} of all carbons were determined (Table 1). The results show that the total pore volume of SEI) the activated carbon exhibiting low-pressure hysteresis) is greater than its ultramicropores volume. This indicates the micropore volume determined from the N_2 adsorption data is the true pore volume, and pore constriction is not significant.[22]

Further insights into the pore structures of the activated carbons can be obtained by using the toluene adsorption data (Figure 2). Similar to the N_2 adsorption isotherms, the toluene isotherms of the activated carbons exhibit a rapid rise in the adsorption amount followed by a plateau characteristic of type I isotherms.[21] The toluene pore volumes of the carbons (Table 1) were determined by using the plateaus of the toluene isotherms. Table 1 shows that the toluene pore volumes, V_{Tol}, of all carbons are very similar and significantly smaller than their corresponding V_{tot}. This is because the N_2 molecule is much

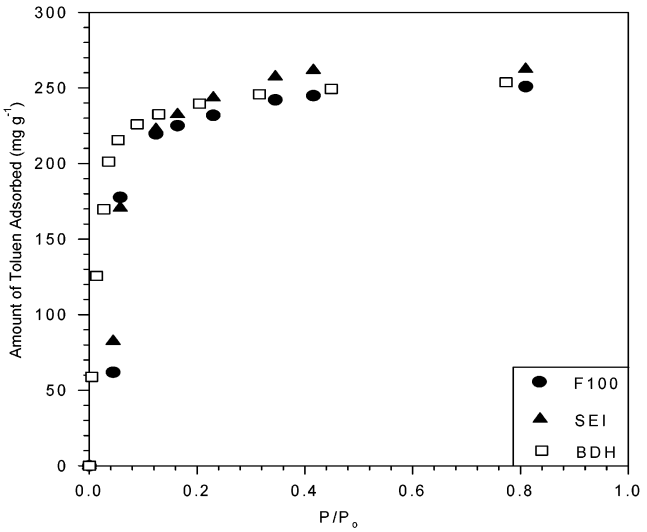

Figure 2. Toluene adsorption isotherms of BDH, SEI, and carbons.

smaller than toluene and can penetrate micropores that are inaccessible to the toluene molecules. Similar observations have also been reported by Marczewska and Marczewski when comparing N_2 and benzene adsorption properties.[32]

The pore structure characterization of the activated carbons shows that even though the total pore volumes of the three carbons are different, their ultramicropore and toluene pore volumes are similar. This indicates that the effect of pore size restriction on the adsorption capacities of the activated carbons is expected to be similar.

4.1.2. Surface Chemistry of the Activated Carbons. Two of the most important surface properties of activated carbons affecting their solution adsorption behavior are their acidity/alkalinity and hydrophilicity. The former affects the extent of the electrostatic and the latter affects the extent of the dispersive interactions, respectively. Generally, hydrophobic activated carbons are basic, high pH_{PZC}. The converse is not true: whereas most hydrophilic activated carbons are acidic, low pH_{PZC}, some surface treatments, such as nitriding, can make the carbon both hydrophilic and basic. For example, nitriding and devolatalizing

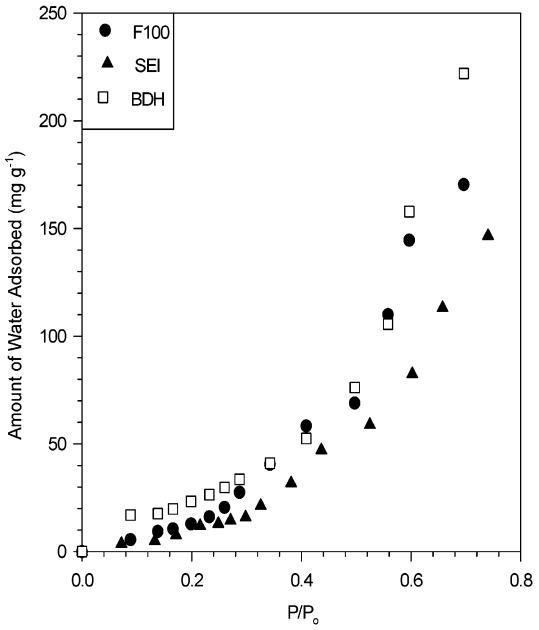

Figure 3. Water adsorption isotherms of BDH, SEI ,and carbons.

TABLE 2: Surface Chemical Characteristics of the Activated Carbons

solute	pH_{PZC}	C (atom %)	O (atom %)	Si (atom %)	S^{2-} (atom %)	Q_0 (mg g^{-1})
BDH	10.2	94.7	5.3			72.5
F100	7.8	94.30	4.90	0.57	0.20	23.8
SEI	9.2	94.7	5.3			22.4

would raise the pH_{PZC} of both carbons. Nevertheless, the latter is found to increase nitrobenzene adsorption, whereas the former is found to be detrimental to its uptake.[16]

The water adsorption isotherms (Figure 3) of the activated carbons were used to compare the hydrophilicity of the activated carbons. The water adsorption isotherms in Figure 3 show low adsorbate−adsorbent interactions in low relative pressures followed by a rapid rise in the adsorption amount in higher pressures, typical of water adsorption onto activated carbon.[21] To compare the hydrophilicity of the three activated carbons, the primary adsorption sites concentrations, Q_0, for each activated carbon was determined using eq 1. The Q_0 values, given in Table 2, show that the order of the hydrophilicity of the carbons is BDH > F100 > SEI, with BDH being significantly more hydrophilic than the other two carbons.

The pH_{PZC} of the activated carbons and their surface elemental analysis determined by XPS, together with their Q_0 values can be used to further characterize their surface functional groups (Table 2). This table shows that the order of the acidity of the activated carbons is F100 > SEI > BDH. It also shows that the surface oxygen concentrations of all carbons are similar. As F100 contains inorganic elements, its surface oxygen concentration cannot be compared with the other two activated carbons. However, the higher alkalinity of BDH than SEI is most likely a result of basic surface oxides, such as chromenes. The presence of such functional groups has been suggested by other researchers.[33−35] BDH and SEI have the same percentage oxygen as determined by XPS analysis. As the pH_{PZC} is higher for BDH, it implies that SEI has a greater number of carboxylic acid groups.

TABLE 4: Correlation Coefficients at pH 2

	molar volume	pK_a	dipole moments	Q' (F100)
Q' (F100)	0.223	0.749	0.692	
Q' (SEI)	0.373	0.984	0.452	0.919
Q' (BDH)	0.540	−0.212	−0.389	0.128
K_m (F100)	−0.840	−0.702	0.288	
K_m S(SEI)	−0.692	−0.589	0.017	
K_m (BDH)	−0.332	0.044	0.936	

4.2. Adsorption of Aromatic Compounds from Dilute Solutions. *4.2.1. Adsorption of Solutes in Molecular Forms.* A number of selected important chemical and physical properties of all solutes used in this work are listed in Table 3. The molecular area in the XZ plane (the long edge) was determined by using the Cerius2 package (Molecular Simulations Inc., San Diego, CA). The molar volumes and the dipole moments of the solutes were calculated using Gaussian98 at model B3LYP/6-31g*.

In this section the relationship between a number of solute parameters with various experimental parameters is examined. Table 4 gives the correlation coefficients tested as discussed in section 2.4.

4.2.1.1. Effects of Carbon Surface Chemistry. The isotherms of all solutes were obtained at pH 2, well below the pK_a of the solutes (Table 3), to investigate the adsorption characteristics of the solutes in their molecular form. All isotherms were then fitted by eq 2a to obtain their corresponding maximum monolayer adsorption capacities and lumped affinity coefficients. The model fit them reasonably well, as demonstrated by Figure 4a,b, showing the isotherms of *p*-cresol and nitrobenzene, respectively.

At pH 2 the fraction of the solutes that is ionized was small; therefore the molecular affinity coefficients, K_m, can be approximated by the lumped affinity coefficients, K_l. The exception is salicylic acid, as the ratio of the anionic to molecular concentrations of salicylic acid is 0.10; therefore, carbon−salicylic acid affinity coefficients are not included in the discussion below.

The K_l values in Table 5 show that the order in the affinity coefficients of the solute carbons are BDH > SEI > F100. As BDH is significantly more hydrophilic than the other two activated carbons, the type of sorbate−sorbent interactions involved could not be the same as those involved in F100 and SEI. The correlation coefficients in Table 4, show that, unlike the other two carbons, the calculated solute dipole moments are significantly correlated with the K_m values of the BDH carbon. The relationships shown in Figure 5 illustrate that the measured affinity coefficients of the solutes for the BDH carbon

TABLE 3: Selected Properties of the Solutes

solute	molecular weight	pK_a	molecular area (Å^2 molecule^{-1}) *XZ* plane	molar volume (cm^3 mol^{-1}) molecular	molar volume (cm^3 mol^{-1}) ionic	dipole moment (Debye) molecular	dipole moment (Debye) ionic
p-cresol	108.1	10.2	26.1	95.53	96.53	1.32	6.53
p-nitrophenol	139.1	7.2	25.1	84.41	91.40	5.45	0.92
benzoic acid	122.1	4.2	24.6	87.19	86.24	2.18	8.89
nitrobenzene	123.1		22.8	90.63	90.63	4.78	4.78
salicylic acid	138.2	2.98	26.7	86.629	95.78	2.20	6.68

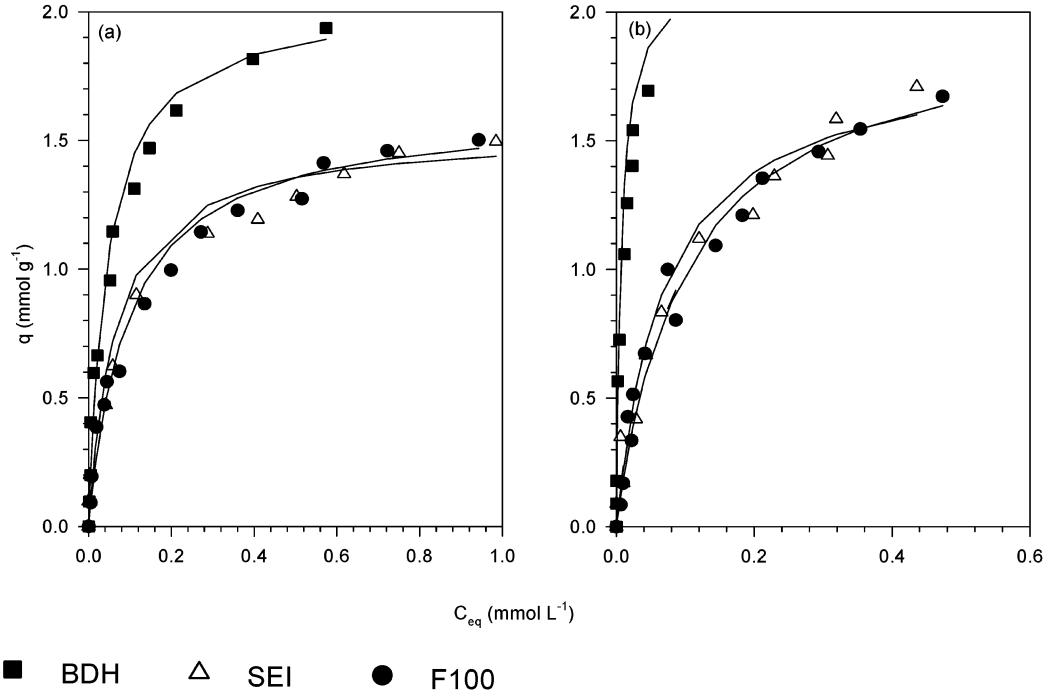

Figure 4. Adsorption isotherms of (a) *p*-cresol and (b) nitrobenzene at pH = 2. Solid lines show the fitted data.

TABLE 5: Langmuir Model Constants Together with the Proposed Values for F100, SEI, and BDH

	affinity coefficients (L mmol^{-1})		monolayer capacity (mmol g^{-1})	
solute	K_l	$K_{l,p}$	Q_{max}	$Q_{max,p}$
		a. For F100		
benzoic acid	19.34	13.7634	1.53	1.46
p-cresol	10.34	14.5372	1.62	1.72
p-nitrophenol	17.81	15.0179	1.71	1.57
salicylic acid	15.76	13.6911	1.438	1.54
nitrobenzene	10.06	15.5812	1.98	
		b. For SEI		
benzoic acid	17.18	24.64	1.47	1.40
p-cresol	15.15	25.62	1.54	1.56
p-nitrophenol	35.42	28.16	1.49	1.47
salicylic acid	51.62	24.53	1.45	1.50
nitrobenzene	14.409	28.85	1.86	
		c. For BDH		
benzoic acid	52.56	39.931	1.92	1.897
p-cresol	22.16	22.31	2.04	1.941
p-nitrophenol	72.50	105.7	1.72	1.899
salicylic acid	13.70	40.32	2.122	2.079
nitrobenzene	136.32	91.96	2.158	

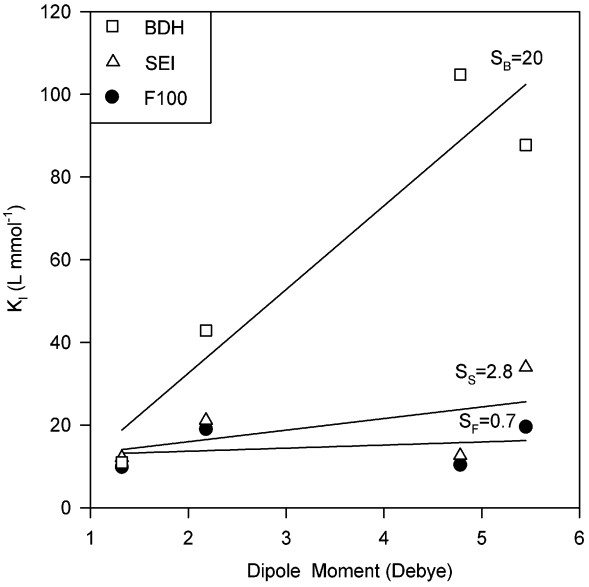

Figure 5. Variation of the K_m values with the dipole moments of the solutes.

increase significantly with the dipole moments of the solutes. In contrast, the corresponding K_m values for the other two carbons do not appear to change significantly with the variation of the dipole moments of the solutes, as is indicated by the slopes of the three plots.

It can therefore be said that in the case of BDH, the dipolar sorbate−sorbent interactions are a significant part of the adsorption forces, whereas for the other two carbons, they are most likely $\pi-\pi$ interactive forces. Table 4 shows that the adsorption capacity of F100, normalized per square meter of the activated carbon (Q'_{max}), appears to correlate with that of the SEI, but not with the Q'_{max} of the BDH. This further indicates that F100 and SEI appear to adsorb in a similar fashion and both behave differently from BDH. This could indicate that part of the observed difference between the hydrophilicity of F100 and SEI is due to the higher fraction of inorganic matter, as was determined by using XPS.

4.2.1.2. Correlation of the Model Parameters. So far, we have shown that the affinity coefficients can be affected by the dipole moments of the solutes. Table 4 shows that molar volumes of the solutes affect the affinity coefficient (K_m) and the solute pK_a affects the uptakes (Q_{max}) of SEI and F100 not BDH. Furthermore, in our previous work,[36] it has been demonstrated that the uptakes of the carbons are strongly affected by the molecular areas in the *XZ* plane.

Table 4 also shows that the linear correlation coefficient of the variation of SEI affinity coefficients with solute molar volumes and the corresponding value of the variation of Q'_{max} values with pK_a is slightly below the significant value ($r = 0.77$) for the given number of data. Nevertheless, the plots of these

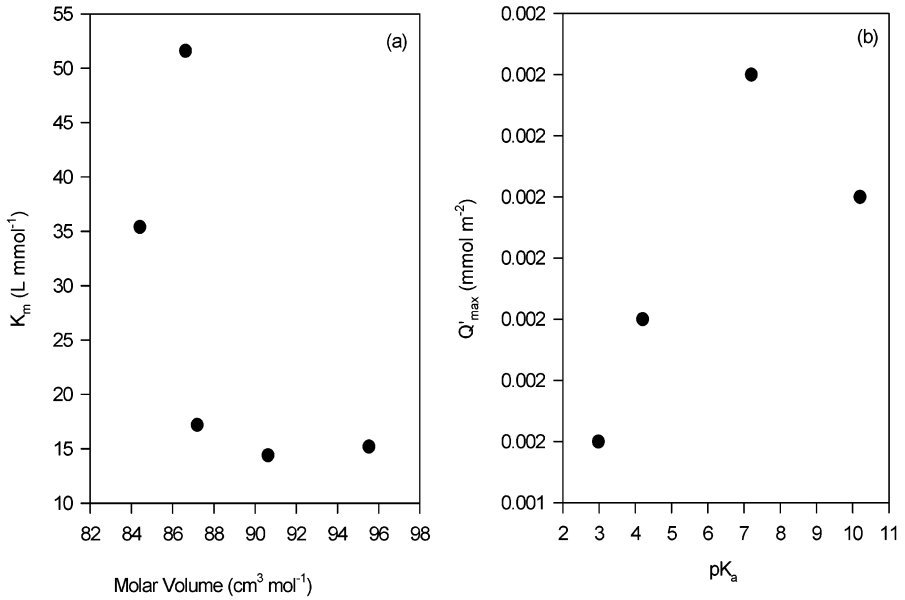

Figure 6. (a) Variation of K_l values of SEI with the molar volumes of the solute and (b) variation of Q'_{max} of F100 with the pK_a of the solutes.

TABLE 6: Fitted F*K* and F*Q* Values of the Activated Carbons

	FK_{MV}	FK_{DM}	FQ_{XZ}	FQ_{pK}
F100	0.507	0.145	0.0543	0.0293
SEI	1.289	0.250	0.547	0.0132
BDH	−0.0438	20.06	0.0792	−0.125

relationships shown in Figure 6a,b indicate that there is a clear relationship between the solute molar volumes and the affinity coefficients of SEI as well as the solute pK_a and the Q'_{max} of F100. Using the effects of these solute parameters, the following models are proposed to correlate the Langmuir constants, K_l and Q_{max} with the relevant solute properties.

(a) Correlation of K_m. The following linear model is proposed for correlating the affinity coefficients of the solutes in their molecular form. The proposed affinity coefficient is noted by $K_{m,p}$. The other variables FK_{MV} and FK_{DM}, represent the contributions of the molar volumes and the dipolar moments, respectively.

$$K_{m,p} = FK_{MV}\cdot MV + FK_{DM}\cdot DM \quad (3)$$

where MV and DM, represent molar volume and dipolar moments, respectively. The parameters FK_{MV} and FK_{DM} are extracted by curve fitting to the experimental data in the second column of Table 5a−c.

(b) Correlation of Q_{max}. The following model for the correlation of the Q_{max} values is proposed, using the area of the molecules in the *XZ* plane and the pK_a of the solutes. The proposed monolayer adsorption capacity is noted by $Q_{max,p}$. The other parameters FQ_{XZ} and FQ_{pK}, representing the contributions of the molecular area and the pK_a, respectively, are then fitted as explained above. The corresponding experimental data are given in the fourth column of Table 5a−c.

$$Q_{max,p} = FQ_{XZ}\cdot XZ + FQ_{pK}\cdot pK_a \quad (4)$$

Using eqs 3 and 4, the Langmuir constants, together with the carbon parameters, FK and FQ were determined and are presented in Tables 5a−c and 6. These tables show that there is strong agreement between the Langmuir Q_{max} values and those calculated using eq 4 ($Q_{max,p}$) for all activated carbons. Furthermore, the proposed affinity coefficients of F100 and BDH appear to be closer to the corresponding Langmuir values, K_m, than those of SEI. This is because (a) there is a significant linear correlation between the dipole moments of the solutes and the BDH affinity coefficients, and (b) there is a significant correlation coefficient between the F100 affinity coefficients and the molar volumes of the solutes. The affinity coefficients of SEI, however, are not significantly correlated with either of the solute parameters.

The proposed affinity coefficients and the maximum uptakes were then used to fit the experimental data into the Langmuir equation. The experimental data, together with the theoretical isotherms using the fitted Langmuir constants and the proposed constants are shown in Figure 7a−d. The solid and the broken lines show the theoretical isotherms, using the fitted and the proposed Langmuir constants, respectively. These figures show that the proposed model for correlating the solute properties to the Langmuir constants fits the data well nearly in all cases, even though the proposed K_l values are not close to those determined from the Langmuir equation. Nevertheless, there are a few cases where the proposed model does not fit the data as well, especially in the high equilibrium concentrations. A closer examination would reveal that in those cases, the fit becomes poorer in high C_{eq}, only when the *XZ* area of the molecule is larger, that is, than the adsorption isotherm of *p*-nitrophenol and salicylic acid onto the BDH surface. This indicates that the proposed model fits the isotherm well in low C_{eq}. However, if geometric restrictions exist, the proposed model does not fit the isotherm as well in higher concentrations.

4.2.2. Adsorption of Ionized Species. In the previous section, it was shown that when adsorption is carried out at a pH well below the pK_a of the solutes, the main adsorption forces are the dispersive and dipolar interactions, with the latter being dominant when basic surface oxides are present. However, when adsorption experiments are carried out at a high pH the presence of the ionic species can alter the adsorption mechanism significantly, as is discussed below.

The experimental data were fitted by eq 2a to obtain the monolayer adsorption capacities, Q_{max}, and the lumped affinity coefficients, K_l, of the adsorption. The experimental data were

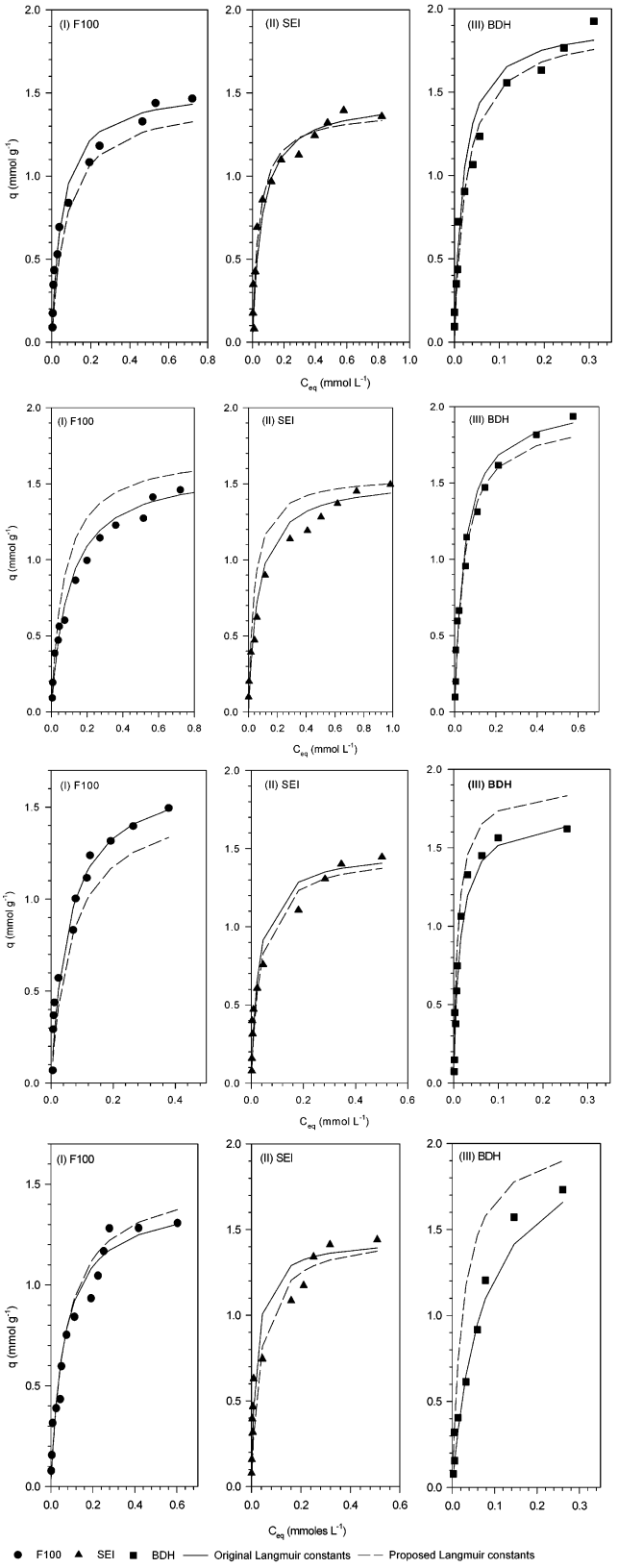

Figure 7. Experimental isotherms of (a) benzoic acid, (b) *p*-cresol, (c) *p*-nitrophenol, and (d) salicylic acid together with the theoretical isotherms using the fitted Langmuir constants and the proposed values.

found to fit the model as shown by the experimental and the fitted isotherms of *p*-cresol and nitrobenzene in Figure 8a,b, respectively. Table 7 shows the correlation between the data sets discussed in this section. The significance of the correlation coefficients is tested as shown in section 2.4.

TABLE 7: Data Sets and Their Corresponding Correlation Coefficients at pH 12

	pK_a	dipole moments	K_m (F100)	Q' (F100)
K_m (F100)	−0.281	−0.338		
K_m S(SEI)	−0.272	−0.726	0.094	
K_m (BDH)	−0.140	−0.166	0.970	
Q' (F100)	0.899	−0.159	0.672	
Q' (SEI)	0.907	−0.158	0.733	0.995
Q' (BDH)	0.924	−0.210	0.640	0.997

Comparison of the solute uptakes of the activated carbons, normalized with respect to their S_{BET} (Q'_{max}), at pH 12 could reveal more insights into the solute-activated carbon interactions (Figure 9). At this pH, all dissociating solutes exist mainly in their ionic form and the equilibrium pH of all sorbate−sorbent systems is the same, regardless of the solute of the carbon type. This figure shows that the uptake of the solutes per unit surface area increases with an increase in the pK_a value of the solutes. Table 7 also shows significant linear correlation coefficients between the solute pK_a values and the corresponding normalized uptakes for all activated carbons.

These observed trends could be explained as follows. At a given solution pH, for solutes that have higher pK_a values, the fraction of the molecular species increases. Because all carbons are negatively charged in such an alkaline solution, the uptake of the solutes with a higher pK_a would be higher on all carbon surfaces, whereas those solutes that have low pK_a values are almost fully ionized at such a high pH. This fact combined with the fact that the activated carbons are negatively charged at this pH, leads to low adsorption capacities for all three activated carbons. The order in Q'_{max} values of nitrobenzene and *p*-cresol of all carbons is closely related to the hydrophobicity of the activated carbons. It can be seen that SEI has the highest value followed by similar values for the other two carbons. This is because the BDH and F100 carbons have higher surface oxygen contents, making them more hydrophilic. As suggested by other authors, the presence of higher surface oxides would lead to more sites being available for water adsorption.[15,37] As a result, lower adsorption per unit surface area is observed for these carbons.

As the anionic fraction of the solute at given pH affects the extent of the electrostatic repulsive forces, the variation of the Q'_{max} values versus pH − pK_a (log α), shown in Figure 10, can give a further understanding of the differences between the solute uptakes of the carbons. The negative part is when the $C_i < C_m$. This shows that when the concentration of the ionic species is smaller than the molecular species, the solute uptake per unit surface area does not change. However, when $C_i > C_m$, the solute uptake decreases very rapidly with the increase in the concentration of the ionic species up to pH − pK_a = 3. Beyond this value, the solute uptake per unit area remains constant. It is also interesting to note that Getzen and Ward reported that beyond this value, the values of the affinity coefficients remained the same.[26]

Another significant difference between the adsorption of the solutes in their ionic and molecular forms can be observed by comparing the K_l values at the two extremes of the pH range. The fitted values of affinity coefficients, K_l, of all solutes at pH 12 are shown in Table 8. The comparison of the lumped affinity coefficients in Table 5 and Table 8 shows that, in the molecular form, the BDH carbon has the highest values of K_m in all cases. However, when the solutes are in their ionic form the values of the lumped affinity coefficients for BDH are the lowest. Equation 2c shows that the K_l values can be approximated to K_i for dissociating solutes except for *p*-cresol, because its pK_a

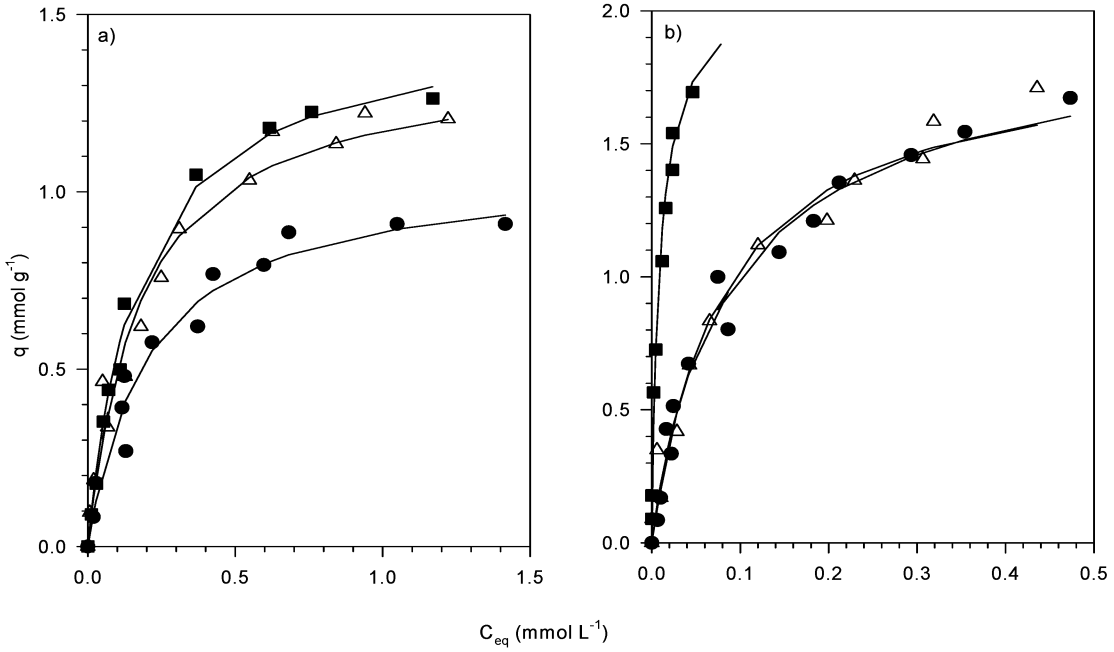

Figure 8. Adsorption isotherms of (a) *p*-cresol and (b) nitrobenzene at pH = 12.

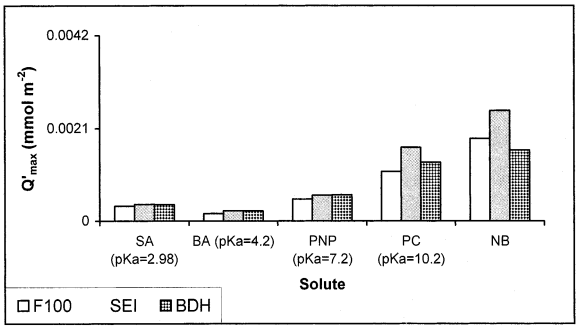

Figure 9. Variation of the solute uptakes per unit surface area of the carbons when the solution pH is 12.

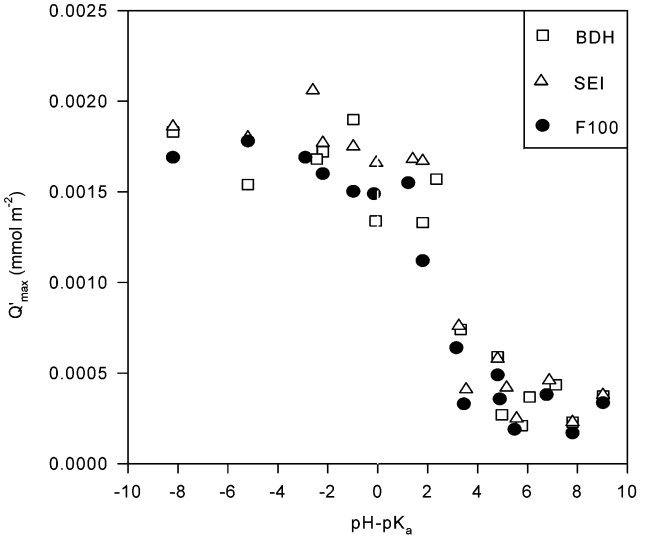

Figure 10. Variation of the solute uptakes per unit surface area of the activated carbons with the log of the ionic fraction of the solutes, (pH − pK_a).

is very high. This indicates that there must be different adsorption mechanisms involved in the two solution conditions. Comparing the correlation coefficients of the Q'_{max} values at pH 2 and 12 (Tables 4 and 7, respectively) also shows that the

TABLE 8: Affinity Coefficients and the Heterogeneity Parameters for All Carbons in Alkaline Solutions

	K_l (L mmol^{-1})		
solute	F100	SEI	BDH
benzoic acid	4.08	5.45	3.44
p-cresol	4.88	5.61	5.86
p-nitrophenol	8.56	13.29	7.08
salicylic acid	8.31	11.65	8.70
nitrobenzene	21.42	7.55	114.61

Q'_{max} of the F100 is only correlated with that of SEI at pH 2. On the other hand, at pH 12, the Q'_{max} values of all carbons are correlated. This indicates that when the solutes are in their ionic form, the adsorption mechanism of all activated carbons may be the same.

The variation of the K_i values with the solute dipole moments (Figure 11) gives further insight into the adsorption mechanism involved at pH 12. Figure 11 shows that with an increase in the dipole of the solutes, the K_i values of the SEI carbon decrease, whereas the trend of the change in the K_i values with dipole moments of the other two carbons is not significant. The lack of a simple relationship between the K_i values and the dipole moments for the more hydrophilic carbons, F100 and the BDH, indicates that the dipolar interactions are not the dominant forces responsible for the observed adsorption behavior. In the case of the more hydrophobic carbon, SEI, the affinity coefficients appear to decrease with an increase in the dipole moments of the solutes. This is not surprising, as an increase in the dipole moment would also indicate an increase in the negative charge of an anion. Therefore, especially when a carbon is hydrophobic, the extent of the interaction would tend to decrease. Another feature of Figure 11 is that the K_i value of salicylic acid−SEI carbon does not fit the same trend as the other solutes. This is expected, because when the pH is 12, K_i is also affected by the concentration of the second ionic species of this compound.

5. Conclusions

Results by various surface characterization techniques in this work showed that the order of the acidity of the carbons was as

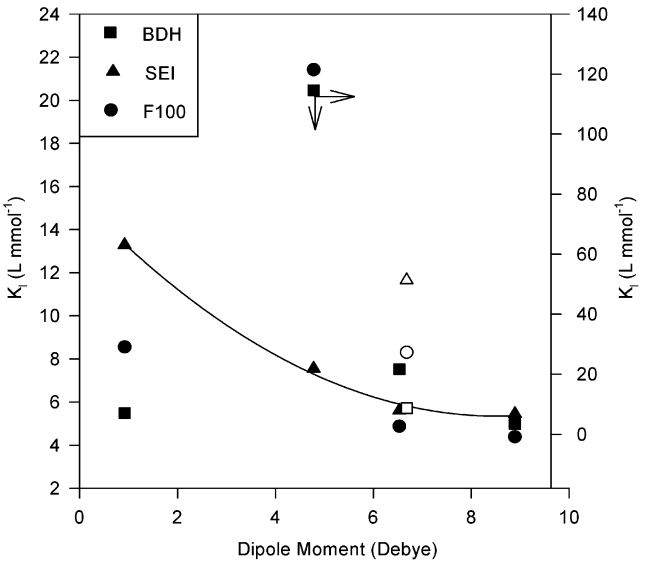

Figure 11. Variation of K_i values with the dipolar moments of the solutes**,**

follows: F100 > SEI > BDH. Furthermore, it was found that the BDH carbon was the most hydrophilic carbon, possibly due to the presence of chromenes.

The dominant adsorption forces involved in the case of the hydrophilic carbon, BDH, were observed to be dipolar interactions, when the solutes were in their molecular forms. On the other hand, $\pi-\pi$ interactions were most likely dominant in the case of the other two carbons. However, when the solutes were in their ionic form, adsorption occurs through nonspecific dispersive forces.

The interaction of aromatic compounds with graphic materials is more complex. The effects of the physical properties of the solutes on the adsorption process were examined by using a proposed linear model to correlate the Langmuir parameters with a few of the significant physical properties of the solutes. The proposed model was found to fit the experimental data well in most cases. However, it is difficult to interpret the physical significance of the fitting parameters, FK and FQ, as only three activated carbons were used in this study. This work demonstrated correlations between adsorbate properties and the adsorption process that challenges our current adsorption models. The task now is to develop a more sophisticated model of the adsorption process that can account for these findings.

References and Notes

(1) Suffet, I. H. *J. Am. Water Works Assoc.* **1980**, *72*, 41.
(2) McGuire, M. J.; Suffet, I. H.; Radzuil, J. V. *J. Am. Water Works Assoc.* **1978**, *70*, 565.
(3) Hsieh, C.; Teng, H. *J. Colloid Interface Sci.* **2000**, *230*, 171.
(4) Leng, C. C.; Pinto, N. G. *Carbon* **1997**, *35*, 1375.
(5) Moreno-Castilla, C.; Rivera-Utrilla, J.; Lopez-Ramon, M. V.; Carrasco-Marin, F. *Carbon* **1995**, *33*, 845.
(6) Laszlo, K.; Nagy, L. G. *Carbon* **1997**, *35*, 593.
(7) Rivera-Utrilla, J.; Utera-Hidalgo, E.; Ferro-Garcia, M. A.; Molina-Castila, C. *Carbon* **1991**, *29*, 613.
(8) Coughlin, R. W.; Ezra, F. S. *Environ. Sci. Technol.* **1968**, *2*, 291.
(9) Ward, T. M.; Getzen, F. W. *Environ. Sci. Technol.* **1970**, *4*, 64.
(10) Mattson, J. S.; Mark, H. B. J.; Malbin, M. *J. Colloid Interface Sci.* **1969**, *31*, 116.
(11) Coughlin, E.; Erza, I. S.; Tan, R. N. *J. Colloid Interface Sci.* **1968**, *28*, 386.
(12) Tamon, H.; Okazaki, M. *Carbon* **1996**, *34*, 741.
(13) Arafat, H. A.; Franz, M.; Pinto, N. G. *Langmuir* **1999**, *15*, 5997.
(14) Halhouli, K. A.; Darwish, N. A.; Al-Dhoon, N. M. *Sep. Sci. Technol.* **1995**, *30*, 3313.
(15) Franz, M.; Arafat, H. A.; Pinto, N. G. *Carbon* **2000**, *38*, 1807.
(16) Radovic, L. R.; Silva, I. F.; Ume, J. I.; Menendez, J. A.; Leon, Y.; Leon, C. A.; Scaroni, A. W. *Carbon* **1997**, *35*, 1339.
(17) Radovic, L. R.; Ume, J. I.; Scaroni, A. W. On Tailoring the Surface Chemistry of Activated Carbons for Their Use in Purification of Aqueous Effluents. *Fundamentals of Adsorption*; Kluwer Academic Publishers: Boston, 1996.
(18) Radovic, L. R.; Moreno-Castila, C.; Rivera-Utrilla, J. Carbon Materials as Adsorbents in Aqueous Solutions. *Chemistry and Physics of Carbon*; PUBLISHER: LOCATION OF PUBLISHER, 2001.
(19) Fleming, I. *Frontier orbitals and Organic Chemical Reactions*; John Wiley and Sons: New York, 1976.
(20) Barradas, R. G.; Hamilton, P. G. *J. Phys. Chem.* **1965**, *69*, 3411.
(21) Gregg, S. J.; Sing, K. S. W. *Adsorptin, Surface Area and Porosity*; Academic Press: London, 1982.
(22) Gardner, J.; Linares-Solano, A.; Martin-Martinez, J. M.; Molina-Sabio, M.; Rodriguez-Reinoso, F.; Torregrosa, R. *Langmuir* **1987**, *3*, 76.
(23) Marsh, H. *Carbon* **1987**, *25*, 49.
(24) *Perry's Chemical Engineering handbook*, 6th ed.; Green, D. W., Maloney, J. O., Eds.; McGraw-Hill Book Co.: New York, 1984.
(25) Barton, S. S.; Evans, J. B.; MacDonald, J. A. F. *Carbon* **1991**, *29*, 1009.
(26) Getzen, F. W.; Ward, T. M. *J. Colloid Interface Sci.* **1969**, *31*, 441.
(27) Miller, J. C.; Miller, J. N. *Statistics for Analytical Chemistry*, 3rd ed.; Ellis Horwood and PTR Prentice Hall: Chichester, U.K., 1993.
(28) Perry, D. L.; Grint, A. *Fuel* **1983**, *62*, 1024.
(29) Ward, R. J.; Wood, B. J. *Surf. Interface Anal.* **1992**, *18*, 379.
(30) Noh, J. S.; Schwarz, J. A. *J. Colloid Interface Sci.* **1989**, *130*, 157.
(31) Rouquerol, F.; Rouquerol, J.; Sing, K. S. W. *Adsorption by Powders and Porous Solids*; Academic Press: London, 1999; Chapter 8.
(32) Derylo-Marczewska, A.; Marczewski, A. W. *Langmuir* **1999**, *15*, 3981.
(33) Cookson, J. T. Adsorption Mechanisms: The Chemistry of Organic Adsorption on Activated Carbon. In *Carbon Adsorption Handbook*; Cheremisinoff, P. N., Ellerbusch, F., Eds.; Ann Arbor Science: Newton, MA, 1978; p 241.
(34) Garten, V. A.; Weiss, D. E. Functional Groups in Activated Carbon and Carbon Black with Ion- and Electron-Exchange Properties. *Proceedings of the Third Conference on Carbon*; Pergamon: New York, 1957.
(35) Garten, V. A.; Weiss, D. E. *Rev. Pure Appl. Chem.* **1957**, *7*, 69.
(36) Haghseresht, F.; Finnerty, J. J.; Nouri, S.; Lu, G. Q. *Langmuir* **2002**, *18*, 6193.
(37) Mahajan, O. P.; Molina-Castilla, C.; Walker, P. L., Jr. *Sep. Sci. Technol.* **1980**, *15*, 1733.